Vietnam Journal of Marine Science and Technology 2025, 25(1) 1–16

Vietnam Academy of Science and Technology

Vietnam Journal of Marine Science and Technology

journal homepage: vjs.ac.vn/index.php/jmst

Localized wind model of Weibull distribution in Vung Tau, Vietnam

Tran Van Chung[1], Nguyen Minh Giam[2], Ho Dinh Duan[3], Nguyen Van Hung[4], Nguyen Huu Huan[1], Phan Minh Thu[1,*]

[1]*Institute of Oceanography, VAST, Vietnam*
[2]*Southern Region Hydrometeorological Center, Ho Chi Minh City, Vietnam*
[3]*Ho Chi Minh City Space Technology Application Center, Vietnam National Space Center, VAST, Vietnam*
[4]*National Remote Sensing Department, Ministry of Natural Resources and Environment, Hanoi, Vietnam*

Received: 10 October 2024; Accepted: 28 November 2024

ABSTRACT

The wind data set of 10 m on the sea surface is provided by Vung Tau Meteorological Station for 2011–2022, with a frequency of 6 h. The purpose of this paper is to find the most effective parameters, that are scale parameter ‘*c*’ and shape parameter ‘*k*’ for the Weibull distribution for the wind regime in Vung Tau based on analyzing and comparing the efficiency of ten numerical methods, namely, the empirical method of Justus (EMJ), the empirical method of Lysen (EML), the method of moments (MoM), the graphical method (GM), the Mabchour’s method (MMab), the energy pattern factor method (EPFM), the maximum likelihood method (MLM), the modified maximum likelihood method (MMLM), the equivalent energy method (EEM), and the alternative maximum likelihood method (AMLM). According to the analysis results, the MLM method is best suited for the wind regimes from February to December; MLM and EMJ methods is best suited for January wind regimes; The AMLM, MLM, and EML methods are best suited for the wind regime in December the MLM and EMJ methods are best suited for November. The MMab method could result in inaccurate forecasting of the wind regime in the Vung Tau area.

Keywords: Weibull distribution, scale parameter ‘*c*’, shape parameter ‘*k*’, wind rose, statistical analysis, Vung Tau.

[*]Corresponding author at: Institute of Oceanography, 01 Cau Da, Nha Trang City 65000, Khanh Hoa, Vietnam. *E-mail addresses*: phanminhthu@vnio.org.vn

https://doi.org/10.15625/1859-3097/22492

INTRODUCTION

The defining characteristic of wind is its variability, both in geographic distribution and over time. This variability spans a broad spectrum of spatial and temporal scales. Wind energy availability increases with the cube of wind speed, making even small speed change significantly impactful due to this cubic relationship. On a global scale, spatial variations highlight the diversity of climates, with some regions experiencing consistently stronger winds than others. These differences are primarily influenced by latitude, which dictates the amount of solar energy received. Within any given climate zone, smaller-scale variations emerge, shaped mainly by natural geographic factors such as the land-to-sea ratio, the size of landforms, and the presence of features like mountains or plains. Vegetation is also crucial in affecting solar radiation absorption and reflection, influencing surface temperature and humidity.

At the local level, topography has a significant impact on wind patterns. Winds are typically stronger on hilltops and mountain peaks than in sheltered areas like leeward slopes or valleys. Additionally, wind speed is noticeably diminished by obstacles like trees or buildings. In ocean hydrodynamic simulations, surface wind is a critical control factor for calculating various air-sea interaction variables, including latent and sensible heat fluxes, carbon dioxide transfer velocity between air and sea, momentum flux, and wind stress on the ocean surface. Wind stress, in particular, is a key parameter integrated into ocean dynamic models, as it plays a fundamental role in shaping the dynamics of air-sea exchanges. Accurately characterizing the local wind regime in a study area is essential to ensure the reliability and effectiveness of simulation outcomes.

Ba Ria-Vung Tau is a coastal province located in Vietnam's Southeast region. To the mainland, it borders Ho Chi Minh City, Dong Nai, and Binh Thuan Provinces, whereas to the east and southeast, it borders the East Vietnam Sea (Bien Dong). This strategic location plays a vital role in the province's socio-economic development, serving as a gateway to the Bien Dong for the surrounding provinces and cities in the Southeast region. The wind patterns in Ba Ria-Vung Tau are notably distinct, shaped by local features such as bays, capes, peninsulas, and islands. Consequently, analyzing the wind dynamics in this region is a challenging task. Leveraging available wind data and employing globally optimized numerical methods to determine the shape and scale parameters of the Weibull distribution is a crucial step in evaluating the impact of wind on the region's complex hydrodynamic processes. These processes are further influenced by the area's winding coastlines, narrow passages, hilly terrain, and elevated areas within the surrounding waters.

Recent findings by Kapen et al. (2020) [1] and earlier studies indicate that up to 10 numerical methods can be utilized to determine parameters for wind speed analysis using the Weibull distribution. In Ba Ria - Vung Tau, the measurement network is relatively extensive, with in-depth surveys conducted through various research projects, providing valuable data for initial modeling conditions. Additionally, studies on wind impacts on currents are well-supported by meteorological stations that directly measure wind effects on the bay. This study employs the most recent dataset, spanning the past 12 years (2011–2022). The selection and calibration of experimental parameters to accurately model wind impacts in this region are critical for refining hydrodynamic models and delivering precise solutions for understanding hydrodynamic processes in the waters of Ba Ria-Vung Tau.

MATERIALS AND METHODS

Materials

The wind dataset were provided by the Vung Tau meteorological station for 12 years, from 2011 to 2022~~.~~ Measurements were recorded every 6 hours at standard meteorological times: 1:00, 7:00, 13:00, and 19:00 h. We conducted a detailed analysis to understand the characteristics of the wind regime in the area.

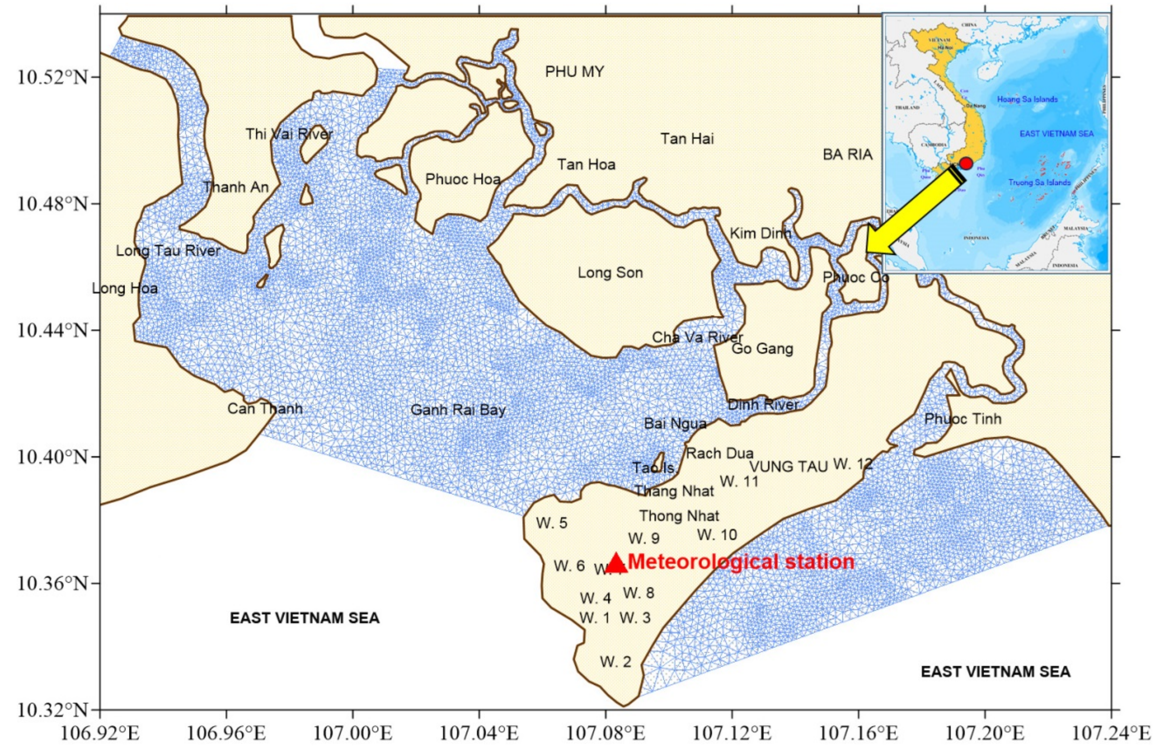

Figure 1. Location of the Vung Tau wind gauge station

Wind data analysis and Weibull parameters estimation

The Weibull distribution is the most commonly used data distribution function for wind due to its better description of wind data than the other distribution functions [2]. The Weibull function has two variations depending on the number of parameters used. However, two parameters (k, c) are mainly used for wind data. If v is the wind speed (m/s), the Weibull probability distribution function, $f(x)$, is expressed as [3–6].

$$f(v)=\frac{k}{c}\left(\frac{v}{c}\right)^{k-1}\exp\left(-\left(\frac{v}{c}\right)^{k}\right) \tag{1}$$

where: c (m/s) and k are the scale Weibull and shape parameters, respectively. The area under the depth of field (DOF) curve the probability density function is called the cumulative distribution function. So, the Weibull cumulative distribution function can be achieved by taking an integral of $f(v)$, denoted by $F(v)$ and given as:

$$F(v)=1-\exp\left(-\left(\frac{v}{c}\right)^{k}\right) \tag{2}$$

In this study, ten methods are discussed, namely, the maximum likelihood method (MLM), the modified maximum likelihood method (MMLM), the method of moments (MoM), the energy pattern factor method (EPFM), the empirical method of Lysen (EML), the graphical method (GM), the empirical method of Justus (EMJ), the Mabchour's method (MMab), the Least square method (LSM), and the alternative maximum likelihood method (AMLM) in order to estimate Weibull parameters for wind energy potential.

Maximum likelihood method (MLM)

This method requires extensive numerical iteration to compute k and c parameter of Weibull function. This method uses a likelihood function of the wind speed data in time series format. The shape (k) and scale (c) parameters are given in [7, 8].

$$k = \left[\frac{\sum_{i=1}^{n} v_i^k \ln(v_i)}{\sum_{i=1}^{n} v_i^k} - \frac{\sum_{i=1}^{n} \ln(v_i)}{n} \right]^{-1}; c = \left(\frac{1}{n} \sum_{i=1}^{n} v_i^k \right)^{\frac{1}{k}} \quad (3)$$

where: n is the number of observations; and v_i is the wind speed measured at the interval i.

Modified maximum likelihood method (MMLM)

When the wind speed data are available in the form of frequency distribution than this method can be applied to obtain Weibull parameter k and c. This method also involves an application of high rated numerical iteration similar to maximum likelihood method. Two Weibull parameters are computed as follows [7, 8]:

$$k = \left[\frac{\sum_{i=1}^{n} v_i^k \ln(v_i) f(v_i)}{\sum_{i=1}^{n} v_i^k f(v_i)} - \frac{\sum_{i=1}^{n} \ln(v_i) f(v_i)}{f(v \geq 0)} \right]^{-1}; c = \left[\frac{1}{f(v \geq 0)} \sum_{i=1}^{n} v_i^k f(v_i) \right]^{\frac{1}{k}} \quad (4)$$

The quantities $f(v_i)$ and f ($v \geq 0$) are the Weibull frequency and the probability of positive wind speed respectively.

Method of Moments (MoM)

Justus and Mikhail [9] suggested the method uses the mean $\bar{v}$ and standard deviation (σ) of wind speeds to determine the Weibull parameter k and c based on the numerical iterative solution of following equations [8, 10–12].

$$\bar{v} = c\Gamma\left(1 + \frac{1}{k}\right); \sigma = c\left[\Gamma\left(1 + \frac{2}{k}\right) - \Gamma^2\left(1 + \frac{1}{k}\right)\right]^{\frac{1}{2}} \quad (5)$$

The mean wind speed $\bar{v}$ and standard deviation (σ) is expressed as:

$$\bar{v} = \frac{1}{n} \sum_{i=1}^{n} v_i; \sigma = \left[\frac{1}{n-1} \sum_{i=1}^{n} (v_i - \bar{v})^2 \right]^{\frac{1}{2}} \quad (6)$$

where: $\Gamma()$ is gamma function and is defined as:

$$\Gamma(x) = \int_0^{\infty} t^{x-1} \exp(-t) dt \quad (7)$$

The gamma function used by Manwell et al., [13] quoting Jamil et al., [14] is given by:

$$\Gamma(x) = \left(\sqrt{2\pi x} \left(x^{x-1}\right).\left(e^{-x}\right).\left(1 + \frac{1}{12}x + \frac{1}{288}x^2 - \frac{139}{51840}x^3 + \ldots\right)\right) \quad (8)$$

MoM is a good substitute, for calculating the shape and scale parameters, to the maximum likelihood method. The shape (k) and scale (c) parameters is computed by the following formula [6, 15]:

$$k = \left(\frac{0.9874}{\frac{\sigma}{\bar{v}}} \right); c = \frac{\bar{v}}{\Gamma\left(1 + \frac{1}{k}\right)} \quad (9)$$

Energy pattern factor method (EPFM)

In this method, the energy pattern factor is used to calculate the Weibull parameters. This factor is needed to be determined first using the average wind speed calculated on the measured data [4, 6], which is given as the ratio of the average of cubed wind speed to the cube of averaged wind speed, given as:

$$E_{pf} = \frac{\overline{v^3}}{\bar{v}^3} \quad (10)$$

where: $\overline{v^3}$ is mean of cube of wind speed and $(\overline{v})^3$ is cube of mean speed. The Weibull shape parameter *k* and scale parameter can be calculated using this formula [8]:

$$k = 1 + \frac{3.69}{E_{pf}^2};\ c = \frac{\overline{v}}{\Gamma\left(1 + \frac{1}{k}\right)} \tag{11}$$

Empirical method of Lysen (EML)

Introduced by Lysen, this method is based on the standard deviation method. The shape parameter '*k*' and scale parameter '*c*' can be computed as follows [2, 4].

$$k = \left(\frac{\sigma}{\overline{v}}\right)^{-1.086};\ c = \overline{v}\left(0.58 + \frac{0.433}{k}\right)^{-\frac{1}{k}} \tag{12}$$

This empirical method can be considered as a special case of the moment method (MoM).

Graphical method (GM)

Graphical method (GM), the least square regression method, is used to interpolate the wind speed data. The cumulative distribution function is to find the values for shape and scale parameters. Eq. (2) is used to compute the respective formulas by taking logarithm twice on both sides and obtaining an equation as [2, 5, 16]:

$$\ln\left\{-\ln\left[1 - F(v)\right]\right\} = k\,ln(v) - k\ln(c) \tag{13}$$

The graphical representation of ln{–ln[1 – *F*(*v*)]} versus ln*v* demonstrates a straight line with a slope of *k* and an intersection with the *x*-axis of (–*k*ln*c*), shape parameter is obtained by the slope of a straight line fitted best to data pairs and the intercept with *y*-ordinate gives scale parameters [10, 17]. Measured wind speed data is used to calculate the values for *x* and *y*; a is the slope, *b* is the intercept, and the standard least square regression method is used to calculate them respectively [2].

$$k = a \text{ and } c = \exp(-b/k) \tag{14}$$

Empirical method of Justus (EMJ)

In the empirical method suggested by Justus, '*k*' is calculated by Eq. (11) same the *Energy pattern factor method* and '*c*' proposed by Justus (EMJ) is given as [2, 18].

$$c = \frac{\overline{v}}{\Gamma\left(1 + \frac{1}{\mathrm{k}}\right)} \tag{15}$$

Mabchour's method (MMab)

This method defines the parameters as [1].

$$k = 1 + \left(0.483(\overline{v} - 2)\right)^{0.51};\ c = \frac{\overline{v}}{\Gamma\left(1 + \frac{1}{k}\right)} \tag{16}$$

Least square method (LSM)

This method is generally useful in engineering and mathematical problems. It assumes a linear correlation between two variables, and after some elite calculation for minimizing relationship, the expression to calculate Weibull parameters can be written as Eqs. (17), (18) [8, 10, 17].

$$k = \frac{n\sum_{i=1}^{n}\ln v_i \times \ln\left[-\ln\left\{1 - F(v_i)\right\}\right] - \sum_{i=1}^{n}\ln v_i \times \sum_{i=1}^{n}\ln\left[-\ln\left\{1 - F(v_i)\right\}\right]}{n\sum_{i=1}^{n}\ln v_i^2 - \{\sum_{i=1}^{n}\ln v_i\}^2} \tag{17}$$

$$c = \exp\left[\frac{k\sum_{i=1}^{n}\ln v_i - \sum_{i=1}^{n}\ln\left[-\ln\left\{1 - F(v_i)\right\}\right]}{nk}\right] \tag{18}$$

Alternative maximum likelihood method (AMLM)

Due to iterative characteristics of maximum likelihood method, a simple calculation procedure has been developed called alternative maximum likelihood method. Equations (19), (20) compute the Weibull scale (k) and shape parameter (c) [1, 8, 11, 17, 18].

$$k = \frac{\pi}{\sqrt{6}} \left[\frac{n(n-1)}{N\left(\sum_{i=1}^{n} \ln v_i^2\right) - \left(\sum_{i=1}^{n} \ln v_i\right)^2} \right]^{\frac{1}{2}} \quad (19)$$

$$c = \left[\frac{1}{n} \sum_{i=1}^{n} (v_i)^k \right]^{\frac{1}{k}} \quad (20)$$

Statistical criteria used for performance evaluation

The following statistical analysis is carried out to evaluate the efficacy of the ten methods: Mean absolute bias error (MABE), Root Mean Square Error test (RMSE), Correlation coefficient (R^2), Chi-Square test (X2), Coefficient of Determination (R2), and Mean Absolute Percentage Error test (MAPE). This test can be summarized as:

Mean absolute bias error (MABE)

The MABE provides the average quantity of total absolute bias error between estimated and observed frequency of wind speed, it is given by [19, 20]:

$$MABE = \frac{1}{n} \sum_{i=1}^{n} |E_i - O_i| \quad (21)$$

where: E_i, O_i are the estimated and observed frequency of wind speed fall into bin i, respectively, and b is the number of bins.

Root mean square error (RMSE)

The RMSE represents the accuracy of distribution by measures the average mismatch between values of observed and estimated frequency of wind speed. It is given by [5, 7, 20–23].

$$RMSE = \sqrt{\frac{1}{n} \sum_{i=1}^{n} (E_i - O_i)^2} \quad (22)$$

High value of RMSE indicates problem, and small value indicates that the distribution is well fitted to data.

Correlation coefficient (R^2)

The coefficient of determination R^2 determines the linear relationship between the calculated values from the Weibull distribution and the calculated values from measured data. A higher R^2 represents a better fit using the theoretical or empirical function and the highest value it can get is 1. R^2 is determined by the Eq. (22) [12, 24–27]:

$$R^2 = \frac{\sum_{i=1}^{n} (E_i - O_i)^2 - \sum_{i=1}^{b} (E_i - O_i)^2}{\sum_{i=1}^{n} (O_i - \bar{O})^2} \quad (23)$$

This criterion describes the correlation between values of estimated and observed frequency of wind speed. The value of varies between 1 (perfect correlation), whereas value of 0 indicates the two data sets are completely different.

Chi-square test (χ^2)

It is a commonly used statistical tool to compare differences between the observed and expected data results and to provide goodness of fit between observed and expected results. The Chi-square test is always testing the state with no momentous difference between the expected and observed result [8, 28].

$$\chi^2 = \sum_{i=1}^{n} \left[\frac{(E_i - O_i)^2}{O_i} \right] \quad (24)$$

The probability distribution is said to be accurate when R^2 is large with least χ^2.

Wind speeds calculated from the Weibull parameters

Weibull parameters extrapolation

If the wind distribution is desired at a height other than the anemometer level, Justus et al., (1978) [9] proposed a consistent methodology that can be used to adjust Weibull c and k (values known at one height) to another desired height.

The Weibull distribution values c_{10} and k_{10} determined at 10 meters height above ground level (AGL), (z_{10} = 10 m) are adjusted to any desired height z by the relation [25, 27, 29, 30]:

$$c_z = c_{10} \times \left(\frac{z}{z_{10}}\right)^n \quad (25)$$

$$k_z = \frac{k_{10}}{1 - 0.00881 \ln(z/10)} \quad (26)$$

where: z and z_{10} are in meters and the power law exponent n is given by:

$$n = [0.37 - 0.088 \ln(c_{10})] \quad (27)$$

Random variables of Weibull distribution

To generate a set of data of Weibull distribution with particular shape and scale parameters, the assumption that the cumulative distribution function for any continuous variable is uniformly distributed in the range of [0, 1] must be considered. Therefore, a random variable having Weibull distribution with a given shape (k) and scale (c) parameter can be generated just by solving the wind speed in Eq. (2) as below [7]:

$$v = c\left[\ln\left(\frac{1}{1-R_n}\right)\right]^{\frac{1}{k}} \quad (28)$$

where: R_n is a random number within [0, 1].

Most probable and maximum energy carrying wind

Likewise, in addition to the average wind speed, there are two other wind speeds called the most probable wind speed (V_{mp}) and maximum energy carrying wind speed (V_{me}), which are also essential for estimating wind energy potential. The most probable wind speed represents a given distribution's most frequently occurring wind speed. After calculating shape and scale parameters, the V_{mp} can be determined as [2, 6, 31].

$$V_{mp} = c\left(1 - \frac{1}{k}\right)^{\frac{1}{k}} \quad (29)$$

V_{me} is an important parameter of wind turbine that should be considered for a site. To get the maximum energy output, it is recommended that the wind machine should be selected with a rated wind speed, which is close to the wind speed, delivering the maximum energy. V_{me} can be computed using the following expression.

$$V_{me} = c\left(1 + \frac{2}{k}\right)^{\frac{1}{k}} \quad (30)$$

RESULTS

Distribution characteristics of available wind speeds

The winds direction and speed analysis results are provided in Table 1, and the Juja wind rose diagram (Fig. 2) for the heights of 10 m above sea level in Vung Tau (2011–2022). Table 1 and Figure 3 show sufficient facts for the frequency of occurrence regarding wind speeds and wind directions. As for wind speeds, the highest frequencies three classes of speeds with of occurrence (over 21%) are mainly in 1 < v_{10} ≤ 2 m/s (occurred 5,987 times, rated 38.6%); 1 m/s < v_{10} (occurred 5,378 times rated 34.7%), and 2 < v_{10} ≤ 3 m/s (occurred 3,178 times rated 20.5%). These most frequent classes of wind speeds are all below 3 m/s, occupying approximately 93.8% of the analyzed data. Recent statistics from UBND Ba Ria-Vung Tau (2023) reveal that the average wind speed ranged from 3 m/s to 5.7 m/s, with Northeast winds averaging 5.2–5.7 m/s and Southwest winds averaging 3–4.1 m/s. The maximum wind speed does not exceed 30 m/s, underscoring stable wind conditions within the area. This data provides critical insights for planning and development initiatives reliant on local wind patterns.

Table 1. Wind speed classification and numbers of occurrences in the data set at 10 m height above sea level in Vung Tau (2011–2022)

Direction	Wind speed (m/s)									Number events	Frequency (%)
	0–1	1–2	2–3	3–4	4–5	5–6	6–7	> 7	Average		
N	213	67	27	3	0	0	0	0	1.4	310	2.0
NNE	159	50	8	2	0	0	0	0	1.2	219	1.4
NE	372	113	21	3	0	0	0	0	1.3	509	3.3
ENE	556	348	138	34	6	0	0	0	1.8	1,082	7.0
E	890	1,360	858	204	19	2	1	0	2.2	3,334	21.5
ESE	669	897	389	40	3	0	0	0	1.9	1,998	12.9
SE	197	118	46	8	4	0	0	0	1.7	373	2.4
SSE	155	105	23	0	0	0	0	0	1.5	283	1.8
S	346	341	150	42	8	1	0	0	1.9	888	5.7
SSW	225	339	171	32	3	1	0	0	2.1	771	5.0
SW	281	625	474	173	38	7	2	1	2.5	1,601	10.3
WSW	259	610	437	130	30	4	2	0	2.4	1,472	9.5
W	303	463	245	69	11	1	0	0	2.1	1,092	7.0
WNW	270	226	111	31	12	1	0	0	1.9	651	4.2
NW	234	189	62	15	3	0	0	2	1.8	505	3.3
NNW	249	136	18	3	1	0	0	0	1.5	407	2.6
Number events	5.378	5.987	3.178	789	138	17	5	3		15,495	
Frequency (%)	34.7	38.6	20.5	5.1	0.9	0.1	0.0	0.0			100.0

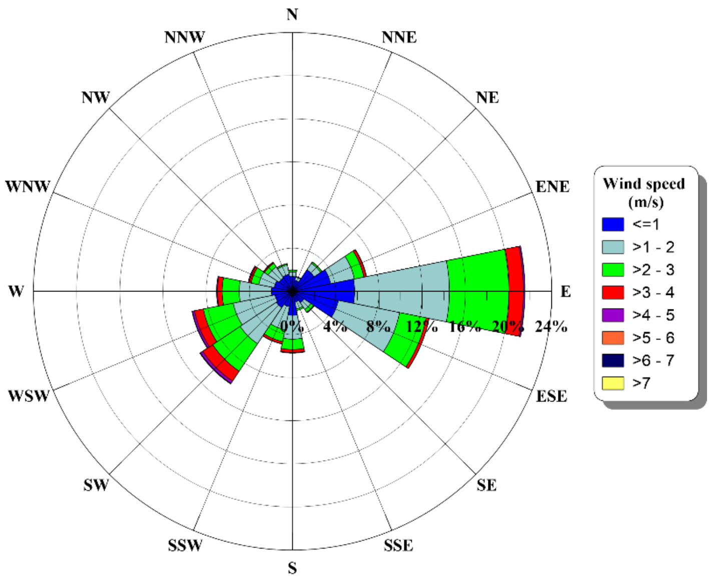

Figure 2. Wind rose diagram at Vung Tau Station (2011–2022)

Regarding the predominant wind directions, the wind regime in the Ba Ria-Vung Tau area is significantly influenced by regional characteristics, as reflected in the frequently occurring wind directions (Fig. 3). Specifically, during the Northeast monsoon season, the Vung Tau area is dominated by three wind directions: E (21.5%), ESE (12.9%), and ENE

(7%). In contrast, the influence of the Southwest monsoon is represented by three wind directions: Southwest (10.3%), West-Southwest (9.5%), and West (7%) (Table 1). Recent data from UBND Ba Ria-Vung Tau (2023) indicates a seasonal variation in wind patterns. In the dry season, the predominant wind direction originated from the Northeast, occurring 30–50% of the time, whereas during the rainy season, winds predominantly come from the Southwest, with a frequency of 60–70%. This understanding of wind direction patterns, influenced by monsoonal changes, is critical for the region's infrastructure planning, environmental management, and renewable energy initiatives in the region. The data reflects the dynamic nature of local wind regimes and underscores the importance of seasonal analysis for effective utilization and preparedness in related sectors.

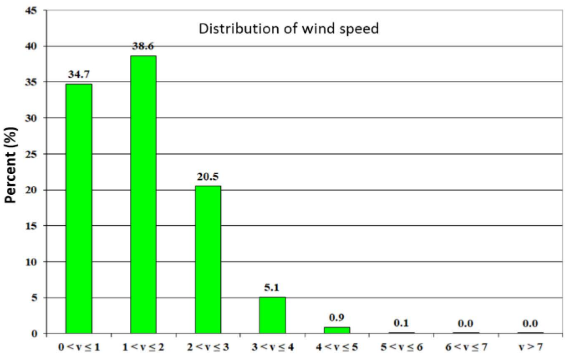

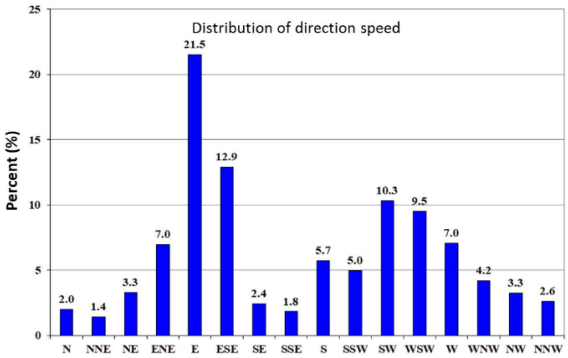

Figure 3. Distribution of wind speed (left) and wind direction (right) in Vung Tau Station

Table 2. Monthly climatology wind speed and the daily peak of wind in Vung Tau Station for 2011–2022

Month	v_{max} (m/s)	α_{max} (^{o})	t_{max}	v_{mean} (m/s)
Jan.	5	E	13 h 31/1/2012	1.5
Feb.	7	E	19 h 27/2/2017	1.9
Mar.	5	E	13 h 08/3/2011	1.9
Apr.	8	NW	13 h 1/4/2012	1.8
May.	7	WSW	19 h 24/5/2016	1.7
Jun.	8	SW	19 h 29/6/2016	1.9
Jul.	7	SW	13 h 16/7/2017	2.1
Aug.	6	W	19 h 28/8/2015	2.1
Sep.	6	WSW	13 h 25/9/2013	1.9
Oct.	6	WNW	13 h 20/10/2016	1.4
Nov.	8	NW	19 h 25/11/2018	1.6
Dec.	6	E	13 h 27/12/2017	1.4

Table 2 presents the monthly climatology of wind speed. The highest monthly mean wind speed is reached to 2.1 m/s in July and August and the minimum ones occur in October and December at 1.4 m/s. However, the daily maximum of wind speeds was occurred at 13 h on April 01, 2012, 19 h on June 29, 2016, and 19 h on November 25, 2018.

Weibull parameters (shape *k* and scale *c*)

Analyses for each method of extracting Weibull parameters were conducted to accurately reflect wind patterns. The results of various distributions, shown as probability density and cumulative distribution compared to observed data by using ten wind analysis methods, are presented in Figure 4. To evaluate the suitability of these methods used, validation criteria were applied, as outlined in Table 3.

Based on the error evaluation results in Table 2 and the monthly and annual charts for the 10 numerical analysis methods, four evaluation criteria were used: Mean Absolute Bias Error (MABE) (The method with the smallest value among the 10 methods was selected); Root Mean Square Error (RMSE) (The method with the smallest value was chosen); Correlation Coefficient (R^2) (The method with the value closest to "1" was selected); and Chi-squared Test (χ^2): The method with the smallest value was chosen. The results indicate that the Maximum Likelihood Method (**MLM**) outperforms other methods in terms of suitability for most months of the year (January to November) and for the annual analysis. For January, the **EMJ** distribution can also be applied. For December, the Adjusted Maximum Likelihood Method (**AMLM**) is recommended. Among the 10 distributions analyzed, the **MMab** distribution consistently failed to meet the criteria for wind analysis in the Ba Ria-Vung Tau area and was deemed unsatisfactory.

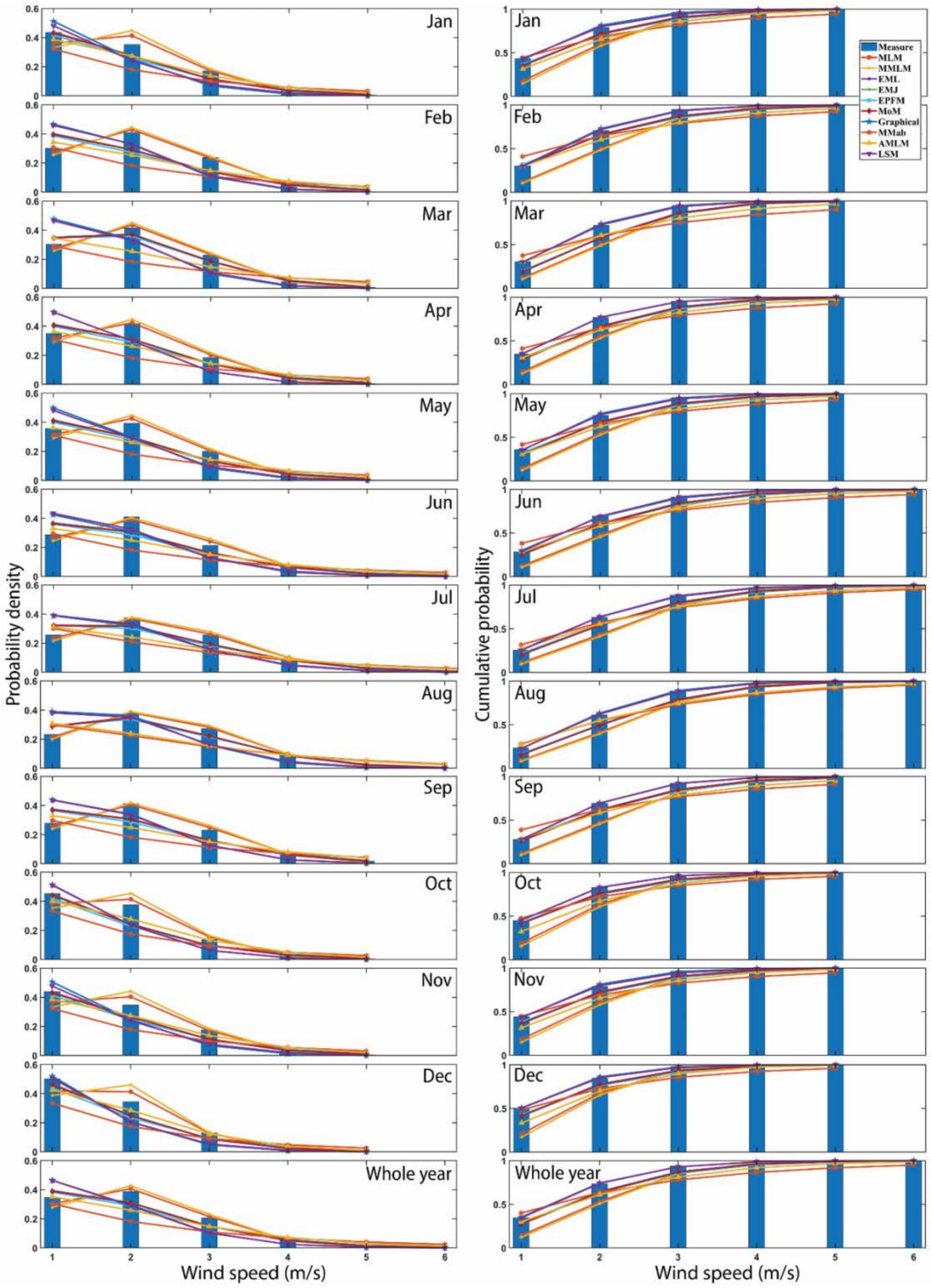

Figure 4. Distribution functions of monthly and yearly wind speed in Vung Tau Station

Table 3. Performance evaluation of the ten selected method at 10 m height above sea level in Vung Tau Station

Month	Parameter	MLM	MMLM	EML	EMJ	EPFM	MoM	Gra	MMab	AMLM	LSM
Jan.	k	**2.253**	2.462	1.553	1.553	1.442	1.539	1.614	***0.986***	1.491	1.496
	c	**2.064**	2.118	1.706	1.720	1.720	1.720	1.448	***1.720***	1.916	1.463
	MABE	**0.028**	0.045	0.029	0.0279	0.037	0.029	0.061	***0.082***	0.040	0.054
	RMSE	**0.095**	0.142	0.098	0.096	0.113	0.097	*0.166*	***0.223***	0.103	0.154
	R^2	**0.938**	0.862	0.934	0.937	0.913	0.935	*0.811*	***0.658***	0.927	0.838
	χ^2	**0.010**	0.022	0.007	0.007	0.011	0.007	0.019	***0.068***	0.011	0.016
Feb.	k	**2.480**	2.600	1.603	1.603	1.486	1.589	1.864	***0.989***	1.387	1.859
	c	**2.314**	2.340	1.896	*1.911*	*1.911*	*1.911*	1.731	***1.911***	2.120	1.757
	MABE	**0.011**	0.018	0.066	0.065	0.070	0.065	0.081	***0.083***	0.069	0.078
	RMSE	**0.036**	0.058	0.183	0.180	0.191	0.181	0.229	***0.265***	0.189	0.218
	R^2	**0.989**	0.971	0.715	0.724	0.689	0.721	0.556	***0.402***	0.697	0.595
	χ^2	**0.001**	0.003	0.035	0.034	0.038	0.034	0.050	***0.078***	0.038	0.046
Mar.	k	**2.505**	2.621	2.047	2.047	1.966	2.035	1.922	***0.993***	1.391	1.863
	c	**2.301**	2.325	2.134	2.149	2.149	2.149	1.718	***2.149***	2.107	1.740
	MABE	**0.011**	0.020	0.028	0.027	0.033	0.028	0.083	***0.085***	0.068	0.079
	RMSE	**0.037**	0.060	0.078	0.074	0.087	0.076	0.231	***0.264***	0.188	0.220
	R^2	**0.989**	0.970	0.949	0.954	0.937	0.951	0.551	***0.415***	0.702	0.594
	χ^2	**0.001**	0.004	0.006	0.006	0.008	0.006	0.051	***0.083***	0.038	0.047
Apr.	k	**2.353**	2.516	1.699	1.699	1.575	1.685	1.766	***0.988***	1.428	1.767
	c	**2.193**	2.232	1.886	1.901	1.901	1.901	1.606	***1.901***	2.019	1.610
	MABE	**0.013**	0.026	0.044	0.043	0.048	0.043	0.078	***0.082***	0.050	0.078
	RMSE	**0.040**	0.073	0.131	0.128	0.145	0.130	0.213	***0.255***	0.164	0.212
	R^2	**0.988**	0.960	0.871	0.877	0.842	0.873	0.658	***0.513***	0.799	0.664
	χ^2	**0.001**	0.005	0.019	0.018	0.023	0.018	0.045	***0.078***	0.029	0.045
May	k	**2.369**	2.527	1.637	1.637	1.522	1.623	1.774	***0.988***	1.428	1.704
	c	**2.198**	2.235	1.848	1.863	1.863	1.863	1.600	***1.863***	2.023	1.623
	MABE	**0.016**	0.029	0.046	0.045	0.049	0.045	0.077	***0.082***	0.048	0.071
	RMSE	**0.054**	0.088	0.131	0.128	0.142	0.130	0.208	***0.241***	0.148	0.195
	R^2	**0.977**	0.938	0.864	0.870	0.841	0.867	0.658	***0.540***	0.828	0.701
	χ^2	**0.003**	0.008	0.017	0.016	0.020	0.017	0.040	***0.068***	0.022	0.035
Jun.	k	**2.300**	2.441	1.678	1.678	1.558	1.665	1.697	***0.992***	1.370	1.790
	c	**2.410**	2.450	2.074	2.090	2.090	2.090	1.832	***2.090***	2.210	1.822
	MABE	**0.012**	0.017	0.042	0.041	0.046	0.041	0.061	***0.066***	0.052	0.062
	RMSE	**0.041**	0.063	0.139	0.137	0.154	0.139	0.193	***0.251***	0.179	0.195
	R^2	**0.988**	0.971	0.856	0.861	0.824	0.857	0.723	***0.532***	0.763	0.717
	χ^2	**0.002**	0.003	0.023	0.022	0.028	0.023	0.041	***0.075***	0.037	0.041
Jul.	k	**2.297**	2.420	1.789	1.789	1.683	1.776	1.739	***1.154***	1.341	1.805
	c	**2.566**	2.604	2.291	2.308	2.308	2.308	1.989	***2.308***	2.347	1.985
	MABE	**0.007**	0.013	0.028	0.027	0.032	0.028	0.048	***0.057***	0.049	0.048
	RMSE	**0.026**	0.048	0.108	0.106	0.122	0.108	0.180	***0.213***	0.179	0.180
	R^2	**0.995**	0.983	0.914	0.918	0.890	0.915	0.761	***0.667***	0.765	0.762
	χ^2	**0.001**	0.002	0.013	0.012	0.017	0.013	0.034	***0.051***	0.036	0.033

Month	Parameter	MLM	MMLM	EML	EMJ	EPFM	MoM	Gra	MMab	AMLM	LSM
Aug.	K	**2.466**	2.560	2.021	2.021	1.943	2.009	1.974	***1.257***	1.333	1.911
	C	**2.593**	2.616	2.403	2.419	2.419	2.419	2.000	***2.419***	2.365	2.032
	MABE	**0.007**	0.013	0.025	0.024	0.028	0.025	0.059	***0.067***	0.064	0.057
	RMSE	**0.023**	0.041	0.083	0.080	0.092	0.082	0.202	***0.212***	0.200	0.192
	R^2	**0.995**	0.985	0.940	0.945	0.926	0.942	0.643	***0.608***	0.650	0.679
	χ^2	**0.000**	0.001	0.007	0.007	0.009	0.007	0.038	***0.051***	0.046	0.036
Sep.	k	**2.401**	2.533	1.676	1.676	1.560	1.662	1.881	***0.991***	1.368	1.860
	c	**2.406**	2.435	2.043	2.059	2.059	2.059	1.828	***2.059***	2.202	1.829
	MABE	**0.013**	0.019	0.055	0.054	0.061	0.055	0.077	***0.081***	0.068	0.077
	RMSE	**0.031**	0.052	0.160	0.157	0.172	0.159	0.208	***0.262***	0.192	0.208
	R^2	**0.991**	0.975	0.758	0.766	0.720	0.761	0.590	***0.351***	0.650	0.591
	χ^2	**0.001**	0.002	0.029	0.028	0.034	0.029	0.045	***0.081***	0.043	0.045
Oct.	k	**2.251**	2.474	1.419	1.419	1.313	1.405	1.556	***0.984***	1.522	1.550
	c	**1.999**	2.055	1.545	1.558	1.558	1.558	1.385	***1.558***	1.860	1.389
	MABE	**0.027**	0.045	0.038	0.038	0.047	0.039	0.060	***0.081***	0.036	0.059
	RMSE	**0.081**	0.131	0.140	0.139	0.157	0.141	0.172	***0.239***	0.112	0.170
	R^2	**0.960**	0.896	0.881	0.883	0.851	0.880	0.821	***0.655***	0.924	0.824
	χ^2	**0.007**	0.018	0.017	0.017	0.023	0.017	0.021	***0.078***	0.014	0.021
Nov.	k	**2.202**	2.426	1.510	1.510	1.393	1.496	1.580	***0.985***	1.494	1.480
	c	**2.062**	2.122	1.682	1.696	1.696	1.696	1.441	***1.696***	1.917	1.457
	MABE	**0.028**	0.043	0.032	0.032	0.042	0.033	0.059	***0.083***	0.041	0.052
	RMSE	**0.094**	0.143	0.105	0.103	0.122	0.105	0.162	***0.222***	0.103	0.152
	R^2	**0.940**	0.861	0.925	0.928	0.899	0.925	0.821	***0.663***	0.928	0.843
	χ^2	0.010	0.023	0.0081	**0.0080**	0.013	0.0084	0.017	***0.068***	0.011	0.015
Dec.	k	2.260	2.506	1.488	1.488	1.371	1.474	1.495	***0.983***	**1.584**	1.458
	c	1.899	1.957	1.519	1.532	1.532	1.532	1.268	***1.532***	**1.777**	1.282
	MABE	**0.032**	0.049	0.037	0.037	0.047	0.038	0.050	***0.086***	0.034	0.046
	RMSE	0.107	0.164	0.112	0.111	0.135	0.114	0.164	***0.246***	**0.100**	0.160
	R^2	0.939	0.859	0.934	0.935	0.904	0.932	0.858	***0.681***	**0.948**	0.865
	χ^2	0.013	0.030	**0.0107**	0.0108	0.019	0.012	0.014	***0.096***	0.013	0.014
Years (2011–2022)	k	**2.291**	2.453	1.694	1.694	1.580	1.681	1.651	***0.990***	1.412	1.678
	c	**2.259**	2.304	1.959	1.974	1.974	1.974	1.658	***1.974***	2.080	1.674
	MABE	**0.013**	0.024	0.031	0.030	0.035	0.030	0.058	***0.069***	0.041	0.057
	RMSE	**0.049**	0.084	0.105	0.102	0.118	0.104	0.186	***0.234***	0.143	0.182
	R^2	**0.984**	0.952	0.926	0.929	0.906	0.927	0.766	***0.631***	0.862	0.776
	χ^2	**0.003**	0.007	0.011	0.011	0.014	0.011	0.033	***0.064***	0.022	0.032

Note: "**Bold**" is the most satisfying and "***italic***" is the least satisfying.

Therefore, a dataset of Weibull distribution parameters (shape k and scale c) has been developed for the Ba Ria-Vung Tau region based on observed data and modeling analysis (Table 4). This dataset is valuable for forecasting wind patterns in meteorological and hydrodynamic models tailored to the area. The monthly Weibull shape parameters, k, at

10 m, were in the range of 1,584–2,505; whereas the monthly Weibull scale parameters, *c*, at 10 m, were in the range of 1,777–2,593 m/s.

Table 4. Monthly Climatology Weibull parameters (shape *k* and scale *c*) for simulating the wind regime in the Vung Tau Station

Month	*k*	*c* (m/s)
Jan.	2,253	2,064
Feb.	2,480	2,314
Mar.	2,505	2,301
Apr.	2,353	2,193
May	2,369	2,198
Jun.	2,300	2,410
Jul.	2,297	2,566
Aug.	2,466	2,593
Sep.	2,401	2,406
Oct.	2,251	1,999
Nov.	2,202	2,062
Dec.	1,584	1,777
All year	2,291	2,259

Discussion

The wind regime in Vung Tau significantly influences the coastal hydrodynamics, affecting currents, wave behavior, and sediment movement. Analyzing localized wind data is crucial for understanding these processes and accurately modeling hydrodynamics. Vung Tau's wind patterns are closely linked to the monsoonal climate, displaying distinct seasonal changes. During the rainy season, typically in transition seasons, southwesterly winds dominate. These winds have an average speed of 2.1 m/s (in July and August) and can reach up to 8 m/s, playing a major role in shaping currents and sediment transport. In contrast, the northeasterly winds less impact the coastal and estuarine circulations. Additionally, diurnal variations driven by land-sea breezes introduce further complexity, influencing the wind patterns and consequently affecting hydrodynamic processes in the region.

However, the observed wind speed data may limit direct use for weather, hydrodynamic, and ecological models. Therefore, it is possible to determine the localized Weibull shape and scale parameters of wind speed. Localized Weibull shape and scale parameters are invaluable for improving the accuracy and efficiency of hydrodynamic and ecological models. The Weibull distribution, characterized by its shape and scale parameters, provides a robust method for modeling wind speed variability in a specific region. Based on observed wind speed data in this study, the Weibull distribution is tested using ten models, which indicate that the MLM method is suitable for most months of the year, whereas the AMLM can be applied in December. The annual *k* and *c* parameters are 2,291 and 2,259 m/s, respectively.

By applying these localized parameters, hydrodynamic models can more accurately predict wind-driven currents, waves, and sediment transport in coastal areas, allowing for better water movement and energy distribution simulations. These enhanced predictions are crucial for understanding erosion patterns, tidal influences, and the impact of winds on coastal infrastructure. Localized wind parameters can also help predict the distribution of nutrients, pollutants, and plankton movements, directly influencing coastal ecosystems through ecological and/or coupled hydro-ecological models. Winds are integral to nutrient exchanges, the spread of contaminants, and the dispersion of marine organisms. By integrating Weibull parameters into these models, predictions about the health and sustainability of coastal ecosystems, such as coral reefs, mangroves, and fisheries, can be more precise, aiding conservation and restoration efforts. Therefore, the findings enhance the accuracy of hydrodynamic models and supports sustainable coastal management practices by providing a deeper understanding of the localized interactions between atmospheric and seawater, ultimately improving predictions and guiding better decision-making for coastal preservation.

CONCLUSION

The analysis of the Ba Ria-Vung Tau wind regime over the past 12 years shows that average wind speeds in the region are predominantly below 3 m/s, accounting for 93.8% of occurrences. This pattern strongly reflects the influence of monsoonal winds. During the northeast monsoon, the region is primarily affected by three wind directions: East (21.5%), East-Southeast (12.9%), and East-Northeast (7.0%). In contrast, the Southwest monsoon is characterized by three main wind directions: Southwest (10.3%), West-Southwest (9.5%), and West (7.0%).

For the annual distribution, based on the 12-year analysis, the MLM method provides the most accurate results, whereas the MMab method produces the least accurate distribution. The shape (*k*) and scale (*c*) parameters are fundamental in simulating the hydrodynamic model in the Ba Ria-Vung Tau coastal waters under the influence of wind regimes across different months, seasons, and inter-seasonal periods. These localized parameters are a critical foundation for understanding the complex interactions between atmospheric forces and marine dynamics. In the context of hydrodynamic models, accurately resolving wind-driven forces is essential for predicting water movement and ecological conditions. The analysis of measured wind data in Vung Tau highlights the significant role of temporal wind variations in influencing estuarine and nearshore processes.

Acknowledgments: The paper was funded by the provincial project "Study on environmental carrying capacity for building up the master plan of sustainable development of aquaculture in Ba Ria-Vung Tau Province".

REFERENCES

[1] P. T. Kapen, M. J. Gouajio, and D. Yemélé, "Analysis and efficient comparison of ten numerical methods in estimating Weibull parameters for wind energy potential: Application to the city of Bafoussam, Cameroon," *Renewable Energy*, vol. 159, pp. 1188–1198, 2020. DOI: 10.1016/j.renene.2020.05.185.

[2] M. K. Saeed, A. Salam, A. U. Rehman, and M. A. Saeed, "Comparison of six different methods of Weibull distribution for wind power assessment: A case study for a site in the Northern region of Pakistan," *Sustainable Energy Technologies and Assessments*, vol. 36, p. 100541, 2019. DOI: 10.1016/j.seta.2019.100541.

[3] I. Ullah and A. J. Chipperfield, "An evaluation of wind energy potential at Kati Bandar, Pakistan," *Renewable and Sustainable Energy Reviews*, vol. 14, no. 2, pp. 856–861, 2010. DOI: 10.1016/j.rser.2009.10.014.

[4] H. Saleh, A. A. E. A. Aly, and S. Abdel-Hady, "Assessment of different methods used to estimate Weibull distribution parameters for wind speed in Zafarana wind farm, Suez Gulf, Egypt," *Energy*, vol. 44, no. 1, pp. 710–719, 2012. DOI: 10.1016/j.energy.2012.05.021.

[5] S. F. Khahro, K. Tabbassum, A. M. Soomro, L. Dong, and X. Liao, "Evaluation of wind power production prospective and Weibull parameter estimation methods for Babaurband, Sindh Pakistan," *Energy Conversion and Management*, vol. 78, pp. 956–967, 2014. DOI: 10.1016/j.enconman.2013.06.062.

[6] M. A. Baseer, J. P. Meyer, S. Rehman, and M. M. Alam, "Wind power characteristics of seven data collection sites in Jubail, Saudi Arabia using Weibull parameters," *Renewable Energy*, vol. 102, pp. 35–49, 2017. DOI: 10.1016/j.renene.2016.10.040.

[7] T. P. Chang, "Performance comparison of six numerical methods in estimating Weibull parameters for wind energy application," *Applied Energy*, vol. 88, no. 1, pp. 272–282, 2011. DOI: 10.1016/j.apenergy.2010.06.018.

[8] P. K. Chaurasiya, S. Ahmed, and V. Warudkar, "Study of different parameters estimation methods of Weibull distribution to determine wind power density using ground based Doppler SODAR instrument," *Alexandria Engineering Journal*, vol. 57, no. 4, pp. 2299–2311, 2018. DOI: 10.1016/j.aej.2017.08.008.

[9] C. G. Justus, W. R. Hargraves, A. Mikhail, and D. Graber, "Methods for estimating

wind speed frequency distributions," *Journal of Applied Meteorology*, vol. 17, no. 3, pp. 350–353, 1978. DOI: 10.1175/1520-0450(1978)017<0350:MFE WSF>2.0.CO;2.

[10] F. George, "A comparison of shape and scale estimators of the two-parameter Weibull distribution," *Journal of Modern Applied Statistical Methods*, vol. 13, no. 1, p. 3, 2014. DOI: 10.22237/jmasm/1398916 920.

[11] T. Arslan, Y. M. Bulut, and A. A. Yavuz, "Comparative study of numerical methods for determining Weibull parameters for wind energy potential," *Renewable and Sustainable Energy Reviews*, vol. 40, pp. 820–825, 2014. DOI: 10.1016/j.rser. 2014.08.009.

[12] P. A. C. Rocha, R. C. de Sousa, C. F. de Andrade, and M. E. V. da Silva, "Comparison of seven numerical methods for determining Weibull parameters for wind energy generation in the northeast region of Brazil," *Applied Energy*, vol. 89, no. 1, pp. 395–400, 2012. DOI: 10.1016/j.apenergy.2011.08.003.

[13] J. F. Manwell, J. G. McGowan, and A. L. Rogers, *Wind Energy Explained: Theory, Design and Application*, 2nd ed., Chichester, UK: Wiley, 2010.

[14] M. Jamil, S. Parsa, and M. Majidi, "Wind power statistics and an evaluation of wind energy density," *Renewable Energy*, vol. 6, no. 5–6, pp. 623–628, 1995. DOI: 10.1016/0960-1481(95)00041-H.

[15] M. Shoaib, I. Siddiqui, Y. M. Amir, and S. U. Rehman, "Evaluation of wind power potential in Baburband (Pakistan) using Weibull distribution function," *Renewable and Sustainable Energy Reviews*, vol. 70, pp. 1343–1351, 2017. DOI: 10.1016/ j.rser.2016.12.037.

[16] Z. H. Hulio, W. Jiang, and S. Rehman, "Technical and economic assessment of wind power potential of Nooriabad, Pakistan," *Energy, Sustainability and Society*, vol. 7, no. 35, pp. 1–14, 2017. DOI: 10.1186/s13705-017-0137-9.

[17] S. A. Ahmed, "Comparative study of four methods for estimating Weibull parameters for Halabja, Iraq," *International Journal of Physical Sciences*, vol. 8, no. 5, pp. 186–192, 2013. DOI: 10.5897/IJPS12.697.

[18] P. K. Chaurasiya, S. Ahmed, and V. Warudkar, "Comparative analysis of Weibull parameters for wind data measured from met-mast and remote sensing techniques," *Renewable Energy*, vol. 115, pp. 1153–1165, 2018. DOI: 10.1016/j.renene.2017.08.014.

[19] K. Mohammadi, O. Alavi, A. Mostafaeipour, N. Goudarzi, and M. Jalilvand, "Assessing different parameters estimation methods of Weibull distribution to compute wind power density," *Energy Conversion and Management*, vol. 108, pp. 322–335, 2016. DOI: 10.1016/j.enconman.2015.11.015.

[20] A. A. Teyabeen, F. R. Akkari, and A. E. Jwaid, "Comparison of seven numerical methods for estimating Weibull parameters for wind energy applications," in *Proc. 2017 UKSim-AMSS 19th Int. Conf. Computer Modelling & Simulation (UKSim)*, Cambridge, UK, 2017, pp. 173–178. DOI: 10.1109/UKSim.2017.31.

[21] S. A. Akdağ and A. Dinler, "A new method to estimate Weibull parameters for wind energy applications," *Energy Conversion and Management*, vol. 50, no. 7, pp. 1761–1766, 2009. DOI: 10.1016/j.enconman. 2009.03.020.

[22] A. A. Teyabeen, "Statistical analysis of wind speed data," in *Proc. IREC2015 The Sixth International Renewable Energy Congress*, Sousse, Tunisia, 2015, pp. 1–6. DOI: 10.1109/IREC.2015.7110866.

[23] T. C. Carneiro, S. P. Melo, P. C. Carvalho, and A. P. D. S. Braga, "Particle swarm optimization method for estimation of Weibull parameters: a case study for the Brazilian Northeast region," *Renewable Energy*, vol. 86, pp. 751–759, 2016. DOI: 10.1016/j.renene.2015.08.060.

[24] A. K. Azad, M. G. Rasul, and T. Yusaf, "Statistical diagnosis of the best Weibull methods for wind power assessment for agricultural applications," *Energies*, vol. 7, no. 5, pp. 3056–3085, 2014. DOI: 10.3390/en7053056.

[25] G. Al Zohbi, P. Hendrick, and P. Bouillard, "Évaluation du potentiel d'énergie

éolienne au Liban," *Revue des Energies Renouvelables*, vol. 17, no. 1, pp. 83–96, 2014. DOI: 10.54966/jreen.v17i1.425.

[26] D. Indhumathy, C. V. Seshaiah, and K. Sukkiramathi, "Estimation of Weibull Parameters for Wind speed calculation at Kanyakumari in India," *International Journal of Innovative Research in Science, Engineering and Technology*, vol. 3, no. 1, pp. 8340–8345, 2014.

[27] D. K. Kaoga, R. Danwe, S. Y. Doka, and N. Djongyang, "Statistical analysis of wind speed distribution based on six Weibull Methods for wind power evaluation in Garoua, Cameroon," *Journal of Renewable Energies*, vol. 18, no. 1, pp. 105–125, 2015. DOI: 10.54966/jreen.v18i1.491.

[28] M. B. H. Kumar, S. Balasubramaniyan, S. Padmanaban, and J. B. Holm-Nielsen, "Wind energy potential assessment by Weibull parameter estimation using multiverse optimization method: A case study of Tirumala region in India," *Energies*, vol. 12, no. 11, p. 2158, 2019. DOI: 10.3390/en12112158.

29] O. S. Ohunakin, M. S. Adaramola, and O. M. Oyewola, "Wind energy evaluation for electricity generation using WECS in seven selected locations in Nigeria," *Applied Energy*, vol. 88, no. 9, pp. 3197–3206, 2011. DOI: 10.1016/j.apenergy.2011.03.022.

[30] A. Mostafaeipour, M. Jadidi, K. Mohammadi, and A. Sedaghat, "An analysis of wind energy potential and economic evaluation in Zahedan, Iran," *Renewable and Sustainable Energy Reviews*, vol. 30, pp. 641–650, 2014. DOI: 10.1016/j.rser.2013.11.016.

[31] A. Keyhani, M. Ghasemi-Varnamkhasti, M. Khanali, and R. Abbaszadeh, "An assessment of wind energy potential as a power generation source in the capital of Iran, Tehran," *Energy*, vol. 35, no. 1, pp. 188–201, 2010. DOI: 10.1016/j.energy.2009.09.009.